PCCP

Accepted Manuscript

ROYAL SOCIETY OF CHEMISTRY

www.rsc.org/pccp

Journal Name

RSCPublishing

COMMUNICATION

Highly Durable Fuel Cell Electrode Based on Ionomer Dispersed in Glycerol

Y. S. Kim[*a], C. F. Welch[b], N. H. Mack[c], R. Hjelm[d], E. B. Orler[±b], M. Hawley[b], K. S. Lee[#a], S.-D. Yim[⊥a], and C. M. Johnston[*§a]

Cite this: DOI: 10.1039/x0xx00000x

Received 00th December 2013,
Accepted 00th December 2013

DOI: 10.1039/x0xx00000x

www.rsc.org/

A major, unprecedented improvement in the durability of polymer electrolyte membrane fuel cells is obtained by tuning the properties of the interface between catalyst and ionomer by choosing the appropriate dispersing medium. While a fuel cell cathode prepared from aqueous dispersion showed 90 mV loss at 0.8 A/cm^2 after 30,000 potential cycles (0.6 - 0.9 V), a fuel cell cathode prepared from glycerol dispersion exhibited only 20 mV loss after 70,000 cycles. This minimum performance loss occurs even though there was over an 80% reduction of electrochemical surface area of Pt catalyst. These findings indicate that proper understanding and control of the catalyst-water-ionomer three-phase interfaces is even more important for maintaining fuel cell durability in typical electrodes than catalyst agglomeration, and this opens a novel path for tailoring the functional properties of electrified interfaces.

Polymer electrolyte membrane fuel cells show promise as a clean and competitive energy source for stationary, automotive and portable applications.[1] A major barrier to their commercialization is the low performance durability of Pt-based electrodes during dynamic fuel cell operation,[2] where frequent and wide voltage changes cause Pt particle growth. The decrease of electrochemically-active surface area (ECSA) of Pt nano-particles is the most obvious reason to blame for the performance loss and consequently, substantial efforts to stabilize Pt particles have been made.[4] However, dynamic fuel cell operations may also induce other structural changes in the electrodes that could cause greater performance loss, particularly in the mass transfer domain.[5] Nonetheless the performance loss associated with electrode structural changes and mitigation strategies are scarce in the literature since i) the structural change of electrodes is concomitant with Pt particle size growth, and ii) changes in ionomeric phase structures are challenging to detect and quantify, making it difficult to decouple those effects.

Here we present novel strategy in improving fuel cell performance durability based on controlling the ionomer structure in dispersion. First, we aimed to investigate the Nafion particle morphology in various solvent systems using small angle neutron scattering (SANS)[6] and discovered that Nafion dispersion particle morphology is much more solvent dependent than had been reported before.[7] When Nafion is dispersed in a water/monohydric alcohol mixture, such as water/2-propanol, a highly solvated, large particulate network structure (> 200 nm in size) with substantial solvent penetration was formed. In contrast, Nafion in aprotic polar solvents, such as N-methylpyrrolidone (NMP), exhibited true solution behaviour forming a random-coil conformation (radius of gyration = 41 Å). Nafion in a polyhydric alcohol, such as glycerol, formed a cylindrical, rod-like structure (radius: 22 Å, cylinder length: 150 Å), with limited solvent penetration. Since Nafion is a commonly used electrode binder in fuel cells, understanding how these dispersing solvents impact the fuel cell electrode performance is critical. Furthermore, this understanding established a framework for further investigations of the relationships among polymer-solvent interactions, solid-state properties of membrane and electrodes prepared from a solution-casting process, and finally electrode performance and durability of altered catalyst-water-ionomer three phase interfaces. The main outcome of this research is strong evidence that supports our initial hypothesis that, in addition to ECSA decrease, ionomer-solvent interactions are important contributing factor to fuel cell durability performance.

Nafion dispersions in three solvent systems were examined: i) water/2-propanol mixture (1:1 volume ratio) that mimics the composition of commercially available dispersions of perfluorinated sulfonic acids;[8] ii) NMP (which is aprotic); and iii) glycerol. The electrode morphology prepared from the dispersing solvents was examined by scanning electron microscopy (SEM) in order to correlate with electrode properties. Membrane electrode assemblies (MEAs) were fabricated in the same manner with the same catalyst and loading, but with ionomer dispersions that differed only in terms of the solvent used. Their performance durability to voltage cycling was compared. The size, distribution and ECSA of Pt nano-particles during voltage cycling was measured from each MEA by transmission electron microscopy (TEM) and cyclic voltammograms,

which revealed the relative importance of catalyst area loss (ECSA) versus transport of ions and oxygen to/from three-phase boundaries (non-ECSA) to the observed performance losses.

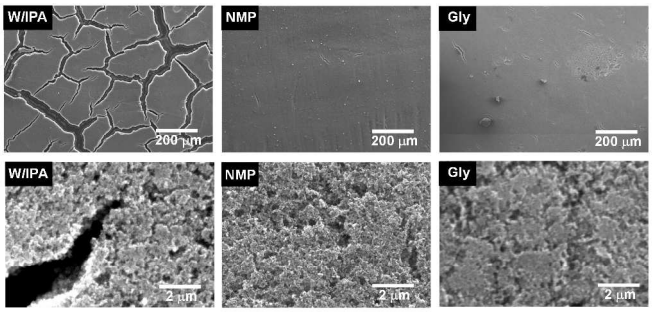

Fig. 1 SEM images of fuel cell electrode prepared from water/2-propanol (W/IPA), NMP and glycerol (Gly) dispersions.

Scanning electron micrograph (SEM) images of the Nafion-bonded Pt/C electrodes exhibited notable differences in microstructure (Fig. 1). The water/2-propanol electrode shows numerous large scale open cracks (> 100 μm), while the NMP electrode exhibits crack-free, yet somewhat coarse microstructure. The glycerol electrode does not have large scale cracks but rather has distributed microcracks (< 10 μm) with a deformed surface. The brittle nature of Nafion cast from water/2-propanol was also observed when casting membranes from the dispersions. The tensile fracture energy of Nafion from water/2-propanol dispersion was only 20 kPa, about 9 times less than that from glycerol dispersion (180 kPa) and about 900 times less than that from NMP dispersion (17.5 MPa) (Fig. S1†). We propose that the poor mechanical properties of Nafion from water/2-propanol originate from the inability to form polymer entanglements or coalescence. According to the best structural fits of the SANS data[6b], water can only ionize the protons of the sulfonic acid groups without solvating the polymer chain. NMP can solvate the polymer chain[6b], allowing polymer chain entanglements to form, which produces tough and ductile films. Although glycerol cannot solvate the polymer chain[6b], it disperses Nafion in the form of very small rod-like micelles – at least two orders of magnitude smaller in size than Nafion in the water/2-propanol dispersion.[6] The small size of the micelles combined with the slow evaporation of glycerol apparently enables polymer mobility to be retained as the film dries so that chain entanglements can form to give an intermediate mechanical strength.

Another aspect of structural differences between electrodes is the time required to relax towards an (pseudo-equilibrium state under conditions relevant to fuel cell operation. This may be important since during steady and dynamic fuel cell operations, fuel cell electrodes are not only exposed to hot and humid environments but also agitated by Pt particle dissolution and agglomeration. Fig. 2 shows the oxygen reduction voltammograms of Pt microelectrodes coated with Nafion prepared from water/2-propanol, NMP and 1,2 propanediol dispersions. The Pt microelectrode prepared from water/2-propanol dispersion reached an equilibrium limiting current (~ 650 nA) within few hours. The Pt microelectrode prepared from NMP dispersion exhibited much slower rate to reach the equilibrium limiting current after 120 h. The Pt microelectrode prepared from 1,2 propanediol, an analogous polyhydric alcoholic solvent to glycerol (see Experimental), on the other hand, started at a lower limiting current (395 nA) and remained the same even after 120 h. Notably, the propanediol derived film exhibits much lower permeability to oxygen. Because oxygen is poorly soluble in water, the accumulation and removal of water from triple phase boundaries is one of the most important factors that limits performance. Although further study is needed to confirm our hypothesis, we suggest that the difference in observed limiting currents is related to the rougher morphology of the water/2-propanol film (see AFM images in Fig. S2†) which allows for water to pool in certain locations rather than forming a more uniform water layer that blocks access of gas-phase oxygen to most of the catalyst surface. An alternate explanation could be that the arrangement of highly hydrophilic sulfonic acid side chains near the catalyst surface as templated by the solvent causes greater or lower local hydrophilicity. Further study will follow after this introductory letter to discriminate between the possibilities.

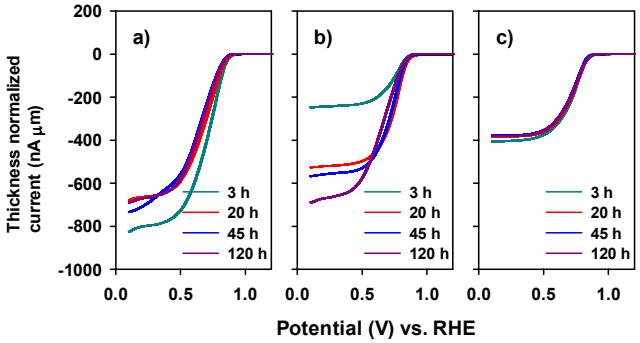

Fig. 2 Oxygen voltammetry change of Pt microelectrodes as a function of time at 40°C, 30% RH; Thin Nafion film cast from (a) water/2-propanol (b) NMP and (c) 1,2 propanediol.

This time-dependent relaxation behaviour was also observed in cast membrane morphology (Fig. S3†).[9] While the membranes cast from water/2-propanol and NMP exhibited enhanced phase separated morphology featured with bright spots after 100°C water vapour exposures, the membrane cast from polyhydric alcohols such as 1,2 propanediol and glycerol did not undergo the morphological change. If one refers back to the structures in dispersion as revealed by SANS[6], the data can be rationalized. The water/2-propanol dispersion generated a Nafion film structure that was created under the influence of water. Therefore, a minor structural shift after introducing water vapour can be expected as water hydrates the hydrophilic side chains. In the case of the film cast from NMP, because NMP solvates both the polymer backbone and side chains during film formation, we can expect a highly homogeneous initial polymer film structure. Upon the introduction of water, however, there will be a new driving force for the hydrophilic side chains to segregate from the polymer backbone. Because this structure is very different from the highly mixed initial structure, it takes time to evolve. As for the 1,2-propanediol film, the Nafion micelles in dispersion have a two-part structure, with a polymer backbone core and a side chain shell[6], because the solvent can penetrate the side chains but not the backbone. Therefore, the side chains are already segregated and the introduction of water does not induce a major reorganization. Another point to consider is why the final state reached by the three films is not the same. It is unlikely that the three films could ever reach the same pseudo-equilibrium state, because under moderate conditions of temperature and without the presence of a good solvent in excess to allow polymer "untangling" and reorganization, e.g., NMP, it would be difficult to physically move the polymer backbones into "ideal" alignment. The relatively short sulfonic acid terminated side chains have sufficient mobility to segregate, but the very long polymer backbones are forced to retain their initial positions with respect to one another with perhaps minor shifting.

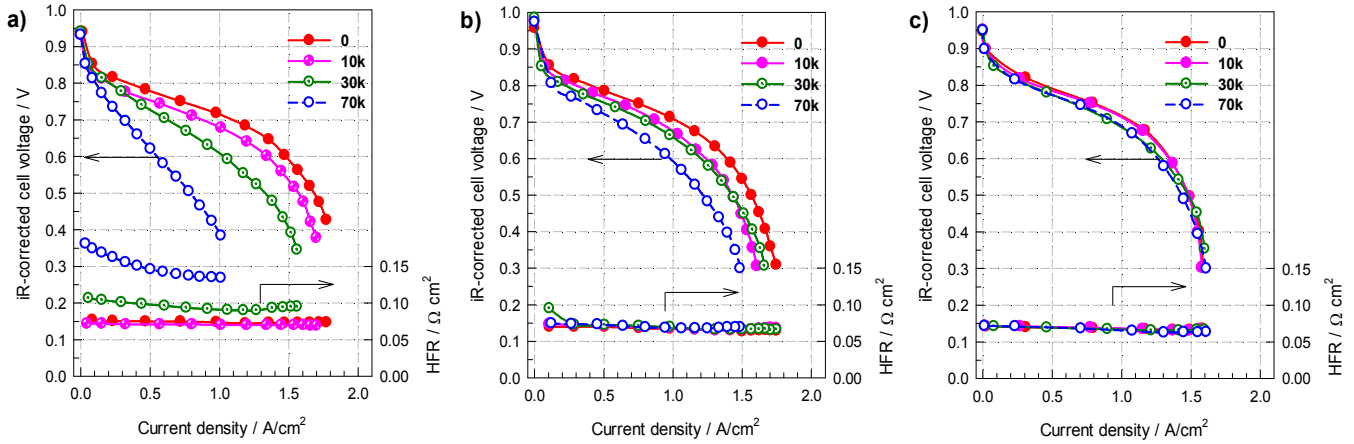

Fig. 3 Fuel cell polarization plots after potential cycling test. (a) water/2-propanol cathode, (b) NMP cathode, and (c) glycerol cathode. iR-corrected polarization curves obtained before cycling (red) and after 10K (pink), 30K (green) and 70K (blue) of potential cycles from 0.6 to 1.0 V under nitrogen conditions. The results presented are obtained on four independent MEAs for each dispersion.

Fig. 3 shows the H_2-air fuel cell initial performance curves and performance durability to voltage cycling using the cathodes prepared from water/2-propanol, NMP and glycerol dispersions. Initial fuel cell performance prepared from the three dispersions was similar when low currents are drawn (e.g. 1.1 A/cm^2 at 0.7 V), where catalytic effects rather than transport controls performance. At high current density, where transport of oxygen and protons are limiting, the water/2-propanol cathode exhibited slightly better performance than NMP and glycerol cathodes (e.g. 1.78 vs. 1.68 vs. 1.58 A/cm^2 at 0.4 V for water/2-propanol, NMP, and glycerol, respectively). Since the high frequency resistance (HFR) values (Fig. 3) were initially the same for all MEAs, we can state that if proton transport is limiting, the effect is localized to triple phase boundary reaction zones and cannot be observed as a drop in total MEA conductivity. We noted from SEM that there are many more electrode cracks in samples prepared from water/2-propanol dispersion than in samples prepared from NMP or glycerol. We propose that this increases the access of gaseous oxygen to the catalyst sites through an indirect effect of cracks on water pooling. As noted before, the location of water in electrodes is critically important because of the poor solubility of oxygen in water. At high current density, water is generated as the product of the oxygen reduction reaction in large quantities. Where this water goes and how quickly is a major determining factor for the MEA performance. Cracks could serve as sinks for water to collect, enabling more of the catalyst sites to remain accessible to gaseous oxygen. The Nafion structure is likely also be "rougher" for the water/2-propanol electrode as discussed above for the microelectrode films, which would amplify this water pooling effect. The higher limiting current obtained with Pt-Nafion microelectrode prepared from water/2-propanol dispersion (Fig. 2) supports this interpretation. (Although a 10 μm film on a microelectrode is not the same as a 3D network of polymer in an electrode with polymer thicknesses ranging 2-10 nm coatings on Pt/C particles to 10s of nm thick "ropes", as observed by TEM, we do expect an analogous influence of solvents on side chain and backbone organization.) Lastly, the side chain structure near the electrode surface could also be different because of the solvent influence, which would affect local hydrophilicity and local proton concentration. Such effects could become important at high current densities. Further study after this short communication is needed to show which of these mechanisms are contributing, and which is dominant.

As for performance durability, the water/2-propanol cathode, exhibited significant performance decreases after the potential cycling test. The performance loss at high current density, i.e., limited by transport processes, in particular was more significant after 30K potential cycling. Concurrent high frequency resistance (HFR) increase suggests a major breakdown of the cathode during the potential cycling test. Considering that Nafion prepared from water/2-propanol is extremely brittle, the electrode breakdown may be related to the detachment of ionomeric binder from catalyst nanoparticles or from the membrane (i.e. membrane-electrode delamination). Similar degradation behaviour accompanied with HFR increase was also observed with membrane-electrode delaminated cells.[10] The performance of the NMP cathode gradually decreased in both the high and low voltage regions with an exception of the high current region between 10K and 30K potential cycles. The lack of additional performance loss in the low voltage region, in contrast to the water/2-propanol electrode, indicates that the performance loss was predominantly affected by ECSA loss. The slight increase in current in the low voltage/high current region after 30K cycles is probably due to the structural change of the cathode toward increasing O_2 permeability, as observed in the microelectrode experiment (Fig. 2b). The performance of glycerol cathode, on the other hand, decreased in the high voltage region but increased in the low voltage region during the potential cycling test. The increased performance in the low voltage/high current density region is possibly caused by Pt particle dissolution and agglomeration during potential cycles, which could assist in opening the electrode structure to O_2 transport. The increased performance in the low voltage region compensated the performance loss in the high voltage even after 70K cycles, and *unprecedented durability improvement was achieved* (ca. 20 mA/cm^2 loss at 0.8 A/cm^2 after 70K potential cycling). The performance durability of glycerol cathode is remarkable when compared with a commercially available MEA which showed 178 mA/cm^2 loss at 0.8 A/cm^2 after 70K potential cycling (Fig. S3†). Considering the data only up to 30K cycles, before the significant breakdown of the water/2-propanol electrode occurs, the stability of the glycerol electrode is still markedly higher than that of the water/2-propanol cathode (90 mV loss) and the NMP cathode (40 mV loss) as well. Although the NMP derived electrode would be expected to have the highest mechanical stability based on the stress-strain results for the solution-cast Nafion membranes, it is important to keep in mind that there is no evidence that the NMP electrode is now mechanically weaker than the glycerol electrode, unlike for the

water/2-propoanol electrode. The water/2-propanol electrode had serious deficiencies in mechanical strength, which led to total decay, but both the NMP and glycerol electrodes exceed the minimum mechanical stability requirement for this test, based on the fact that neither electrode caused a change in the HFR, which would decrease if polymer pathways had degraded. Therefore, it is not inconsistent that the glycerol electrode has better performance durability than the NMP electrode, but it simply indicates that once the mechanical stability requirement has been satisfied, other factors become important.

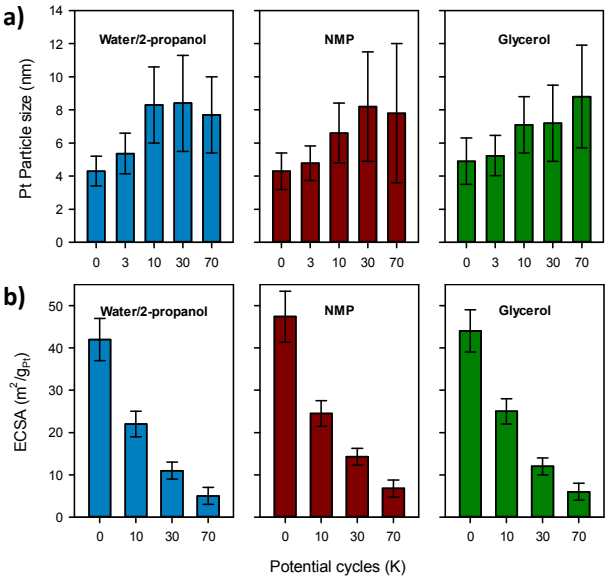

Fig. 4 (a) Pt particle size and (b) ECSA change of Pt particles for the cathodes prepared from three dispersions; The error bar in pt particle size denotes particle size distribution.

The most obvious factor to consider first is whether there is a difference in the electrochemical surface areas found in the different types of electrodes over time. This particular cycling test was originally designed by US DOE to evaluate catalyst degradation,[11] due to the generally accepted belief that Pt particle growth and consequent ECSA decrease would be the primary source of electrode performance loss after potential cycling between 0.6 and 1.0 V. Based on this assumption, one would expect that since the performance is very different between the cathodes after 70K potential cycles, then the Pt particle size distribution should also differ significantly. Fig. 4a shows the change of Pt particle size and spatial distributions (denoted as the error bar) for all three cathodes during the potential cycling test, indicating that the changes in particle size and distribution do not depend on dispersing solvent but depend on the number of potential cycles. Fig. 4b shows that ECSA of all three cathodes (obtained from H_2 desorption peak of cyclic voltammograms of the cathodes) decreased in a similar manner after each cycling step from 45 m^2/g for 0K cycles to 23 m^2/g for 10K cycles, to 12 m^2/g for 30K cycles and 6 m^2/g for 70K cycles. These results with additional information on Pt size distribution (Fig. S4†) and Pt particle morphology (Fig. S5†) indicate that the Pt particle growth and consequent ECSA decrease are not the primary cause for the performance durability of these cathodes contrary to the prevailing opinion. Furthermore, a major change of Pt particle size and distribution occurred between 0K and 10K potential cycles (Fig. 4a), whereas major fuel cell performance changes took a place after 10K potential cycles (Fig. 3). These observations imply that fuel cell performance is largely governed by the catalyst/polymer/solvent interactions, rather than just the ECSA of Pt nano-particles. Note that the fuel cell performance using the glycerol cathode after 70K potential cycles was comparable to the initial performance, yet the performance was achieved with only 14% of initial ECSA, which suggests that maintaining ECSA of Pt catalyst is not crucial for respectable fuel cell performance.

Yet another aspect of durability must be considered -the long term quality of the triple-phase boundaries. The improved performance durability of the glycerol cathode is perhaps related to the time-dependent stability observed in the microelectrode and AFM experiments. A possible mechanism is the following: when the electrode inks are made, for both NMP and glycerol, likely the sulfonic acid terminated polymer side chains are attracted to the oxide/hydroxide covered Pt surface, which creates a good triple-phase interface for the Pt particles in both types of electrode, at least initially. However, as the Pt particles grow from ~4 nm to ~8 nm, the original polymer coating is disturbed. Therefore, new polymer-catalyst interfaces must be formed with whatever polymer segments are near the Pt surfaces. In the glycerol derived electrode, every part of the Nafion polymer was uniformly templated to have segregated side chains, because the Nafion micelles in glycerol have segregated side chains. Therefore, it is easy for a side-chain rich polymer-platinum interface to reform. However, in NMP-derived electrodes, aside from the polymer in direct contact with the Pt particles, there is a tendency for the polymer backbones and side chains to be mixed. Once the Pt particle grows or changes position, the chances that it comes in contact with Nafion that has the ideal segregated structure is lower. Even though the glycerol-derived Nafion should be mechanically weaker than NMP-derived Nafion, its polymer structure is more uniformly suitable to form good triple-phase boundaries as the platinum particles grow, which we propose as the reason for its better durability. Additionally, the glycerol-derived electrode is less porous than the NMP-derived electrode (Fig. S6†), across all pore sizes from 1- 35 nm. This may increase the chance that the Pt particles can form more complete triple-phase boundaries as they grow, i.e., they do not grow into empty spaces without the opportunity to encounter polymer side chains.

This is a seeding study that opens a new venue in fuel cell research and points out importance for detailed understanding of these highly complex catalyst-water-ionomer interfaces that are so strongly influenced by solvent. The mechanisms of the interactions remains to be investigated, however, it is noteworthy to mention that a unique ionomer network structure along with the increase of particle size bring beneficial synergy that leads to increased durability performance. Moreover, Pt particle size agglomeration that leads to the increase in specific activity[4a] is equally present for all three solvent systems presented here. For that reason, the increase in particle size and consequently higher specific activity of the catalyst cannot be assigned as the only factor for improved durability. Based on the results presented here, it is obvious that control of the polymer structure in electrodes can offer unprecedented benefits in tuning the fuel cell performance regardless of dramatic ECSA losses.

In conclusion, we prepared fuel cell cathodes from three dispersing solvents in order to investigate the structural effect on performance durability during potential cycling test. Our novel electrode structure derived from Nafion-glycerol interaction makes it possible to avoid significant performance loss during potential cycling, even with 86% reduction of electrochemical surface area. While recent efforts to address fuel cell performance loss have focused on preventing Pt particle growth, a hypothesis presented here is that microstructure of the electrode dictated by

polymer/solvent interactions largely determines fuel cell performance durability. Possible mechanisms for the differences are proposed in the text. Additional investigations into the relationships between dispersion morphology and other electrode components are necessary to more precisely address the role of dispersing solvents.

Experimental

The water/2-propanol Nafion dispersion was prepared by conventional dispersing technique in a closed vessel.[12] 89.5 g of water, 70.5 g of 2-propanol, and 4 g of Na^+-form Nafion® 212 membrane were placed in a 200 ml closed vessel; solid content was 2.5 wt%. The vessel was heated in a heat mantle at 210°C for 3 h. The internal vessel pressure was about 500 psi. A transparent liquid dispersion was obtained without residual solid polymer. The solvent ratio of water to 2-propanol for concentrated dispersions was measured from ^{1}H NMR technique. NMP and glycerol Nafion® dispersions were prepared by the Los Alamos National Laboratory-developed direct dispersing technique.[13] 0.5 g of the Na^+-form Nafion® 212 membrane was cut into small pieces and placed in a 60 ml vial with 20 g of glycerol; solid content was 2.5 wt%. The vial was heated in a convection oven at 110°C (NMP) or 210°C (glycerol) for 3 h. A clear brown-colored liquid solution was obtained without residual solid polymer. ^{1}H NMR of glycerol dispersion indicates that no side reaction or degradation occurs during the dispersion process.[6a]

SEM images of the electrodes prepared from water/2-propanol (W/A), NMP, and glycerol (Gly) dispersion. Electrodes were prepared from decal painting of catalyst inks using the dispersions, followed by drying at 140°C. Membrane electrodes were mounted on carbon tape and then imaged normal to the membrane surface.

MEAs were prepared. Commercial Nafion® dispersion (Ion Power Inc.) was used for anode electrode binder. Fuel cell electrodes were prepared from commercial carbon-supported Pt (E-TEK catalyst) and the Nafion® dispersions described above. 0.0625 g of 20% Pt/C (20% carbon supported Pt, E-TEK catalyst) was added to 1 g of Nafion® dispersion (commercial, water/2-propanol, NMP or glycerol dispersion) in a 20 ml vial with stirrer. This mixture was stirred extensively for at least 8 h. To this mixture, 0.025 g of tetrabutylammonium hydroxide was added for water/alcohol dispersion catalyst inks and further stirred at least 1 h. Catalyst inks were prepared by painting with a camelhair brush onto decal substrates. Active area of MEAs was 5.0 cm^2 with a catalyst loading of 0.20 mg/cm^2. Painted electrodes were placed in an oven at 140°C until dry, as determined by a stable mass reading. Electrodes were transferred from the substrates to membranes by hot pressing at 210°C for 10 min. Salt-form MEAs were acidified by immersion in boiling 0.5 M aqueous sulfuric acid for 2 h, followed by treatment with boiling deionized water for 2 h. The MEA was dried at 75°C under vacuum for 30 min before the cell assembly. H_2/air fuel cell performance of the MEAs was measured at 80°C using a fuel cell test station (Fuel Cell Technologies). Fully humidified H_2 and air were supplied at a rate of 200 and 500 sccm for both anode and cathode, respectively (backpressure of 30 psig). Initial cell break-in was conducted at a constant cell voltage of 0.7 V for 14 h at 80°C. The *iR*-corrected polarization curves were obtained from initial and after 3K, 10K, 30K and 70K potential cycles. Potential cycling from 0.6 to 1.0 V with a scanning rate of 50 mV/s. was performed using a potentiostat under fully humidified H_2/N_2 conditions.

Microelectrode experiment was performed with thin Nafion film cast from different dispersions. The working electrode was a 100 μm diameter platinum microdisk electrode (Bioanalytical Systems). The actual surface area of the microdisk was determined from hydrogen adsorption measured by cyclic voltammetry in a 0.5 mol dm^{-3} H_2SO_4. The roughness factor determined from the hydrogen adsorption charge was around 1.7. Thin Nafion films (thickness = 4-9 μm) cast on the electrode by depositing a small volume (typically 8 μl) of 2.5% Nafion dispersion prepared above. The electrode was then turned placed in an oven at 80°C. Due to the high boiling point of glycerol, 1,2 propanediol dispersion was used instead. The drying time was 24 h. No effect of the drying time on the results of electrochemical measurements was found. Detail set-up for the microelectrode experiment was described previously.[14]

Pt particle size and distribution of the MEAs were estimated from TEM images by measuring the average circular diameter of several hundred (>200) particles. ECSA of Pt particles was measured from the hydrogen desorption region of cyclic voltammograms. Voltammetry measurements were carried out intermittently at 30°C using humidified H_2 at the anode (~50 sccm) and humidified N_2 (~200 sccm) at the cathode with a sweep rate of 50 mV/s.

Acknowledgments

We thank the U.S. Department of Energy Fuel Cell Technologies program for funding this work. We thank Jerzy Chilistunoff for microelectrode experimental set-up. We thank Andrea Labouriau for NMR measurement. We thank Karen More (ORNL) for assisting TEM measurement. K.S.Lee acknowledges the research grant from Gwangju Institute Science and Technology. S.-D.Yim acknowledges the support from Korea Institute of Energy Research. Los Alamos National Laboratory is operated by Los Alamos National Security LLC under DOE Contract DE-AC52-06NA25396.

Notes and references

[a] Sensors and Electrochemical Devices Group, [b] Polymers and Coatings Group, [c] Physical Chem. & Applied Spectroscopy Group, [d] Los Alamos Neutron Science Center, Los Alamos National Laboratory, Los Alamos, NM 87545, USA. E-mail: yskim@lanl.gov; cjohnston2005@gmail.com.

† Electronic Supplementary Information (ESI) available: Figures S1-S6, mechanical properties of solution cast Nafion, microscopic images of membranes, electrode analysis using TEM and BET. See DOI: 10.1039/c000000x/

± Current address: Department of Chemistry, Virginia Tech. Blacksburg, VA 24060.

§ Current address: Robert Bosch LLC, Research and Technology Center North America, 4005 Miranda Ave., Palo Alto, CA 94304.

Graduate research associate from School of Materials Science and Engineering, Gwangju Institute Science of Technology.

⊥ Visiting scholar from Hydrogen and Fuel Cell Department, Korea Institute of Energy Research.

1 L. Schlapbach, *Nature*, 2009, **460**, 809.

2 R. Borup, J. Meyers, B. Pivovar, Y. S. Kim, R. Mukundan, N. Garland, D. Myers, M. Wilson, F. Garzon, D. Wood, P. Zelenay, K. More, K. Stroh, T. Zawodzinski, J. Boncella, J. E. McGrath, M. Inaba, K. Miyatake, M. Hori, K. Ota, Z. Ogumi, S. Miyata, A. Nishikata, Z. Siroma, Y. Uchimoto, K. Yasuda, K. I. Kimijima, N. Iwashita, *Chem. Rev*., 2007, **107**, 3904.

3 J. A. Gilbert, N. N. Kariuki, R. Subbaraman, A. J. Kropf, M. C. Smith, E. F. Holby, D. Morgan, D. J. Myers, *J. Am. Chem. Soc*., 134, **36**, 14823; J. C. Meier, C. Caleano, I. Katsounaros, A. A. Topalov, A. Kostka, F. Schuth, K. J. J. Mayrhofer, ACS Catalysis, 2012, **2**, 832; D. Myers, X. Wang, N. Kariuki, R. Subbaraman, R. Ahluwalia, X.

Wang, 2011 US DOE Hydrogen and Fuel Cells Program and Vehicle Technologies Program, Washington D.C. May 9-13, 2011.

4 H. A. Gasteiger, S. S. Kocha, B. Sompalli, F. T. Wagner, *Appl. Catal., B* 2005, **56**, 9; P. J. Ferreira, G. J. la O', Y. Shao-Horn, D. Morgan, R. Makharia, S. Kocha, H. A. Gasteiger, *J. Electrochem. Soc.*, 2005, **152**, A2256; H. R. Colon-Mercado, B. N. Popov, *J. Power Sources*, 2006, **155**, 253; J. Zhang, K. Sasaki, E. Sutter, R. R. Adzic, *Science*, 2007, **315**, 220; Y. Y. Shao, G. P. Yin, Y. Z. Gao, *J. Power Sources*, 2007, **171**, 558.

5 M. F. Mathias et al., *Electrochem. Soc. Interface*, 2005, **14**, 24.

6 C. Welch, A. Labouriau, R. Hjelm, B. Orler, C. Johnston, Y. S. Kim *ACS Macro Lett*., 2012, **1**, 1403; Y. S. Kim, Lecture 23, Advances in Materials for Proton Exchange Membrane Fuel Cell systems, Feb. 17-20, 2013, Pacific Grove, California.

7 P. Aldebert, B. Drefus, M. Pinery, *Macromolecules*, 1986, **19**, 2651; P. Aldebert, B. Dreyfus, G. Gebel, N. Nakamura, M. Pinery, F. Volino, *J. Phys. (Paris)* 1988, **49**, 2101; B. Loppinet, G. Gebel, C. E. Williams, *J. Phys. Chem. B,* 1997, **101**, 1884.

8 *Product literature for DuPont™ Nafion dispersion*, http://www2.dupont.com/FuelCells/en_US/products/nafion.html

9 M. E. Hawley, Y. S. Kim, R. P. Hjelm, *MRS Symp. Proc*. 2010, **1213**, T02-09.

10 B. Pivovar, Y. S. Kim, *J. Electrochem. Soc*., 2007, **154**, B739; Y. S. Kim, M. Einsla, J. E. McGrath, B. S. Pivovar, *J. Electrochem. Soc.*, 2010, **157**, B1602; Y. S. Kim, B. S. Pivovar, *J. Electrhochem. Soc.*, 2010, **157**, B1616.

11 *DOE Cell Component Accelerated Stress Test Protocols for PEM Fuel Cells,* http://www1.eere.energy.gov/hydrogenandfuelcells/fuelcells/pdfs/component_durability_profile.pdf, 2009

12 W. G. Grot (Du Pont), US Patent 4,433,082, 1984.

13 Y. S. Kim, K. S. Lee, T. Rockward, US Patent 7,981,319, 2011; Y. S. Kim, K. S. Lee, T. Rockward, US Patent 8,236,207, 2012

14 J. Chlistunoff, F. Uribe, B. Pivovar, *ECS Transactions*, 2006, **1**, 137; J. Chlistunoff, *J. Power. Sources*, 2014, **203**, 245.

